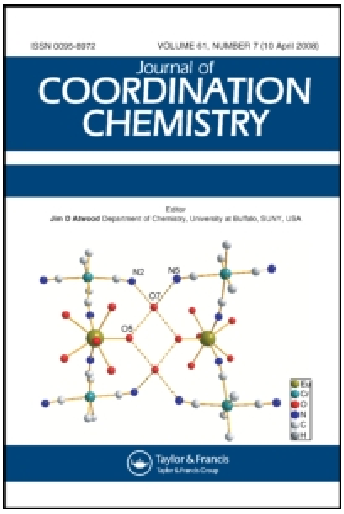

Journal of Coordination Chemistry

Publication details, including instructions for authors and subscription information:
http://www.informaworld.com/smpp/title~content=t713455674

Octahedral Co(II) and Ni(II) complexes of Schiff bases, semicarbazone and thiosemicarbazone, synthesis, biological, spectral, and thermal studies

Khlood S. Abou-Melha[a]
[a] Scientific Departments, Department of Chemistry, Education College for Girls, Assir, Abha, Saudi Arabia (KSA)

To cite this Article Abou-Melha, Khlood S.(2008) 'Octahedral Co(II) and Ni(II) complexes of Schiff bases, semicarbazone and thiosemicarbazone, synthesis, biological, spectral, and thermal studies', Journal of Coordination Chemistry, 61: 13, 2053 — 2067

To link to this Article: DOI: 10.1080/00958970701862167

URL: http://dx.doi.org/10.1080/00958970701862167

Journal of Coordination Chemistry
Vol. 61, No. 13, 10 July 2008, 2053–2067

Taylor & Francis
Taylor & Francis Group

Octahedral Co(II) and Ni(II) complexes of Schiff bases, semicarbazone and thiosemicarbazone, synthesis, biological, spectral, and thermal studies

KHLOOD S. ABOU-MELHA*

Scientific Departments, Department of Chemistry, Education College for Girls, Assir, Abha, Saudi Arabia (KSA)

(*Received 18 May 2007; in final form 12 June 2007*)

A new series of cobalt(II) and nickel(II) complexes, $[M(ligand)(H_2O)_2(Y)]$ $(M = Co(II)$ or $Ni(II)$; $Y = Cl^-$, Br^- or $NO_3{}^-)$, containing the Schiff-base semicarbazone and thiosemicarbazone, HL^1 and HL^2, formed from 4-hydroxycoumarin-3-carbaldehyde have been synthesized. The nature of bonding and the stereochemistry of the complexes have been deduced from elemental analyses, infrared, electronic spectra, magnetic susceptibility, and conductivity measurements. An octahedral geometry has been suggested for the complexes. The metal complexes were screened for their antifungal and antibacterial activities on different species of pathogenic fungi and bacteria and their biopotency has been discussed.

Keywords: Schiff bases; Semicarbazone; Thiosemicarbazone; 4-Hydroxycoumarin-3-carbaldehyde; Antifungal; Antibacterial

1. Introduction

Several coumarin derivatives have pronounced medicinal value as antibacterial and antifungal agents [1–7]. Others display antitubercular activity [8] or show insecticidal properties [9]. These compounds have important pharmaceutical value because of their anticoagulant and antitumor activities [10–13]. Generally, *in vitro* structure-activity relationship studies have shown that cytotoxicity is found with derivatives containing ortho-dihydroxy substituents. Also, the chemical-structure/biological activity study of the coumarins showed that the addition of a cathecolic group to the basic structure induces increased cytotoxic activity in tumor cell lines [14–16]. Preparation of potential biologically active compounds today is predominantly based on combination of different substructures which increased the biological activity of known active substances. This study is based on the fact that 4-hydroxycoumarin derivatives possess anticoagulant activity while aminothiazole derivatives of 4-hydroxy-coumarins possess significant antibacterial and antifungal activity. The different cytotoxic values found for the coumarins could be related to the presence and the positions of the hydroxyls in their structures. On the other hand, thiosemicarbazones are well established as sulfur

---

*Email: khold_melha@yahoo.com

Journal of Coordination Chemistry
ISSN 0095-8972 print/ISSN 1029-0389 online © 2008 Taylor & Francis
DOI: 10.1080/00958970701862167

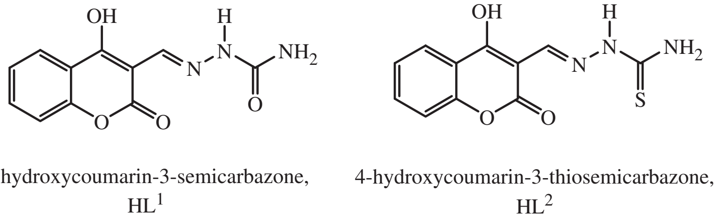

Figure 1. Structures of $\mathbf{HL^1}$ and $\mathbf{HL^2}$.

donor ligands for transition metal ions [17–21], with remarkable biological activities related to their metal complexing ability. These compounds present a variety of biological activity ranging from antitumor, fungicide, bactereocide, antiinflammatory, and antiviral activities [22–24]. The chelating behavior, spectral properties and coordination modes of thiosemicarbazones having pyrazolone as NNS donor have been previously examined [25, 26].

In the present work, we report the synthesis, infrared and electronic spectra, magnetic susceptibility, and conductivity measurements, as well as antibacterial and antifungal properties of cobalt(II) and nickel(II) complexes containing Schiff bases HL^1 or HL^2 derived from 4-hydroxycoumarin-3-carbaldehyde (figure 1).

2. Experimental

2.1. *Materials*

Chloride, bromide and nitrate salts of Co(II) and Ni(II) were obtained from BDH. Semicarbazide, hydrochloride, thiosemicarbazide, *o*-hydroxyacetophenone, N-bromosuccinamide, phosphorus oxychloride, acetic and hydrochloric acids were either from BDH or Merck. Organic solvents were reagent grade.

2.2. *Synthesis of the ligands*

2.2.1. Synthesis of chromon-3-carbamide. Chromon-3-carbamide was synthesized in two steps as follows [27].

1. *Synthesis of chromon-3-carbaldehyde*. *o*-Hydroxyacetophenone (27.2 g, 200 mmol) was dissolved in 120 mL DMF. To this solution, phosphorous oxychloride (50 mL, 600 mmol) was added gradually. The reaction mixture was stirred under cooling (ice-bath), left for an hour, allowed to reach room temperature, left for 24 h and then poured onto an ice-water mixture with stirring until complete precipitation. The obtained chromon-3-carbaldehyde was filtered off, washed with 5 mL cold distilled water and finally recrystallized from methanol and then dried over anhydrous $CaCl_2$ for 24 h (m.p. 152°C, 83–89%).

2. *Synthesis of chromon-3-carbamide*. Under inert conditions and in the presence of 500W light source (lamp), N-bromosuccinamide (3.7 g, 23 mmol) was added gradually

to a solution of chromon-3-carbaldehyde (3 g, 17.3 mmol) dissolved in 130 mL carbon tetrachloride. The reaction mixture was further stirred at 0°C for an hour. Concentrated ammonia solution (10 mL) was added with vigorous stirring. The reaction mixture was left under stirring for another hour, then poured onto 10% acetic acid. The precipitate formed was filtered off, washed with a mixture of methanol-carbon tetrachloride and recrystallized from methanol to yield yellow crystals (m.p. 140°C, 86%).

2.2.2. Synthesis of 4-hydroxycoumarin-3-carbaldehyde (I). The preparation was carried out according to the previously reported method [27]. Chromon-3-carbamide (6.4 g, 20 mmol) was added gradually to a solution of KOH (200 mL, 1M). The mixture was stirred for 15 min then acidified with conc. HCl until complete precipitation. The precipitated solid was filtered off, washed with 10 mL distilled water, 5 mL ethanol and finally diethyl ether, and then recrystallized from petroleum ether, **100–120** (yield 84%; m.p. 137°C).

2.2.3. Synthesis of 4-hydroxycoumarin-3-semi-(HL^1) and thiosemicarbazone (HL^2). The ligands were prepared by the following general method. Semi- or thiosemicarbazide (10 mmol) dissolved in 10 mL hot distilled water was added to a hot solution of **(I)** (10 mmol) dissolved in 10 mL ethanol. The reaction mixture was further stirred for 15 min, allowed to cool and the precipitate formed was filtered off, washed with 5 mL cold distilled water and finally recrystallized from acetic acid, and dried over anhydrous $CaCl_2$ for 24 h. The formed golden yellow to yellow crystals of semicarbazone (yield 73%; m.p. 260°C) and thiosemicarbazones (yield 80%; m.p. 210°C), respectively, were collected and stored.

2.3. *Preparations of the metal complexes*

A general method has been used for the preparation of complexes using reaction of metal salts and the corresponding Schiff base in molar ratio ($M:L = 1:1$). Metal salt (3 mmol dissolved in 10 mL ethanol) was heated on a water bath to ensure complete dissolution. To this solution, the ligand (3 mmol dissolved in 10 mL ethanol) was added gradually. The reaction mixture was refluxed for 3 h with constant stirring. The brown or deep brown precipitate was filtered off, washed several times with 50% (v/v) ethanol–water mixture to remove any traces of unreacted starting materials, then washed with diethyl ether and dried in a vacuum desiccator over $CaCl_2$. The obtained solid metal complexes and their colors are shown in table 1. The complexes are stable solids, decomposing above 230°C without melting and insoluble in ether, acetone, ethanol, methanol and chloroform; however, they are soluble in DMSO and DMF.

2.4. *Physical measurements and analyses*

Carbon, hydrogen, nitrogen and sulfur microanalyses were carried out at the analytical center of King Khalid University, Assir, Abha, Saudi Arabia using a Perkin Elmer 2400 Series analyzer. Analyses of the metals followed decomposition of their complexes with concentrated nitric acid. The resultant solution was diluted with distilled water and filtered to remove the precipitated ligand. The solution was

Table 1. Analytical, conductivity, and magnetic data of Co(II)and Ni(II) complexes of **HL¹** and **HL²**.

Compound (F. Wt.)	Yield (%)	Elemental analysis, Found/(Calcd)% C	H	N	Anion	S	Metal	Ω_M (Ohm cm^2 mol^{-1})	μ_{eff} (B.M.)
HL¹ $C_{11}H_9N_3O_4$ (247)	75	53.91 (53.44)	4.11 (3.64)	19.58 (17.00)	–	–	–	–	–
(**1**) $[Co(L^1)(H_2O)_2(Cl)]$ $C_{11}H_{12}N_3O_6ClCo$ (367.5)	53	35.42 (35.06)	3.55 (3.19)	11.31 (11.16)	10.01 (9.43)	–	16.11 (15.67)	3.2	4.8
(**2**) $[Co(L^1)(H_2O)_2(Br)]$ $C_{11}H_{12}N_3O_6BrCo$ (421)	45	31.12 (31.35)	3.21 (2.85)	10.32 (9.98)	8.36 (8.43)	–	14.43 (14.01)	2.4	4.9
(**3**) $[Co(L^1)(H_2O)_2(NO_3)]$ $C_{11}H_{12}N_4O_9Co$ (403)	50	32.55 (32.75)	3.23 (2.98)	13.53 (13.90)	–	–	14.54 (14.64)	1.8	2.6
(**4**) $[Ni(L^1)(H_2O)_2(Cl)]$ $C_{11}H_{12}N_3O_6ClNi$ (376.2)	47	35.48 (35.09)	3.51 (3.19)	10.75 (11.16)	9.66 (9.44)	–	15.36 (15.60)	2.3	2.8
(**5**) $[Ni(L^1)(H_2O)_2(Br)]$ $C_{11}H_{13}N_3O_6BrNi$ (420.7)	44	31.31 (31.38)	3.41 (2.85)	10.11 (9.98)	8.32 (8.44)	–	14.25 (13.95)	1.9	3.0
(**6**) $[Ni(L^1)(H_2O)_2(NO_3)]$ $C_{11}H_{12}N_4O_9Ni$ (402.7)	46	32.55 (32.78)	3.23 (2.98)	13.73 (13.91)	–	–	14.64 (14.58)	2.2	2.9
HL² $C_{11}H_9N_3O_3S$ (263)	80	50.64 (50.19)	3.25 (3.42)	15.58 (15.97)	–	12.58 (12.17)	–	–	–
(**7**) $[Co(L^1)(H_2O)_2(Cl)]$ $C_{11}H_{12}N_3O_5SClCo$ (392.5)	55	34.12 (33.63)	3.46 (3.06)	10.33 (10.70)	9.44 (9.04)	8.53 (8.15)	15.43 (15.03)	2.4	5.3
(**8**) $[Co(L^1)(H_2O)_2(Br)]$ $C_{11}H_{12}N_3O_5SBrCo$ (437)	40	29.73 (30.21)	3.13 (2.75)	9.42 (9.61)	8.34 (8.12)	7.73 (7.32)	13.91 (13.50)	1.8	4.8
(**9**) $[Co(L^1)(H_2O)_2(NO_3)]$ $C_{11}H_{12}N_4O_8SCo$ (419)	53	32.01 (31.50)	3.23 (2.86)	13.11 (13.37)	–	7.43 (7.62)	14.23 (14.08)	2.3	4.9
(**10**) $[Ni(L^1)(H_2O)_2(Cl)]$ $C_{11}H_{12}N_3O_5SClNi$ (392.2)	47	34.12 (33.66)	3.52 (3.06)	11.12 (10.71)	9.45 (9.05)	(8.16)	15.55 (15.04)	1.9	2.9
(**11**) $[Ni(L^1)(H_2O)_2(Br)]$ $C_{11}H_{13}N_3O_5SBrNi$ (436.6)	46	30.71 (30.23)	3.11 (2.75)	9.25 (9.62)	8.54 (8.13)	7.65 (7.33)	13.83 (13.51)	2.2	3.1
(**12**) $[Ni(L^1)(H_2O)_2(NO_3)]$ $C_{11}H_{12}N_4O_8SNi$ (418.7)	48	31.23 (31.53)	4.22 (2.87)	13.12 (13.37)	–	7.54 (7.63)	15.22 (14.9)	2.3	2.7

then neutralized with aqueous ammonia and the metal ions titrated with EDTA [28]. Electronic spectra were recorded for the solutions of the ligands in ethanol, and for Co(II) and Ni(II) complexes as Nujol mulls on a Shimadzu UV–Vis spectrophotometer model 1601 in the range 190–1100 nm. IR spectra were recorded in KBr/CsI discs using FT-IR-4000 and FT-IR 1650 Perkin Elmer spectrometers in the range 200–4000 cm^{-1}. ^{1}H NMR spectra were carried out at room temperature in DMSO-d_6 and tetramethylsilane (TMS) as an internal reference using a Perkin Elmer 1340 spectrophotometer. The halides were estimated by Volhard's method [28]. Magnetic susceptibilities of the complexes were measured by the Gouy method at room temperature using a model MK1 Johnson Matthey Alpha Products magnetic susceptibility balance. The effective magnetic moments were calculated using the relation ($\mu_{\mathrm{eff}} = 2.828\ (\chi_m T)^{1/2}$ B.M., where χ_m is the molar susceptibility corrected using Pascal's constants for diamagnetism of all atoms in the compounds. The TG-DSC measurements were carried out on a Shimadzu thermogravimetric analyzer in dry nitrogen and a heating rate of 10°C min^{-1} using the TA-50 WS1 program. Mass spectra were recorded at 70 eV and 300°C on a MS 5988 Hewlett-Packard mass spectrometer. Conductivity measurements were measured in DMF solutions of the complexes (10^{-3} M) using a model LBR, WTWD-812 Wilhelm conductivity meter fitted with a model LTA100 cell.

2.5. *Screening of antibacterial and antifungal activities*

The *in vitro* evaluation of antimicrobial activity was performed according to the diffusion technique [29, 30]. Bacteria, including *Staphylococcus aureus* and *Escherichia coli*, were grown in nutrient broth at 37°C for 24 h. *Candida albicans* and *Fusarium solani* were grown in malt broth at 28°C for 48 h.

The ligand/complexes were tested using the diffusion technique [29, 30] on solid media. Sterile (5 mm) diameter sensitivity discs were impregnated with different concentrations of the ligand/complex (50 µg or 100 µg mL^{-1}) in DMF. Discs of each tested compound were laid onto nutrient agar for bacteria or potato dextrose agar for fungi. Plates are surface spread with 0.2 mL of logarithmic phase bacteria or fungi cultures. A 0.5 mL spore suspension (10^8 spores/mL) for bacteria or for filamentous fungi was also spread onto potato dextrose agar plates. The plates were then incubated for 24 h at 37°C for bacteria and 48 h at 28°C for fungi. Additionally, antibiotic discs for Cephalosporin and Streptomycin are tested as positive controls. The results were recorded by measuring the zones of growth inhibition surrounding the discs.

3. Results and discussion

3.1. *Schiff-base ligands, HL^1 and HL^2*

The Schiff-base ligands, HL^1 and HL^2, are expected to be pentadentate ligands with coordination sites of coumarin-carbonyl, thio-keto or carbonyl-oxygen, azomethine-nitrogen, imine-nitrogen and phenolic-oxygen. Comparison of the IR spectra of the ligands and their metal complexes indicate that the Schiff bases are monobasic

Table 2. ^{1}H NMR data of the ligands in DSO-d$_6$.

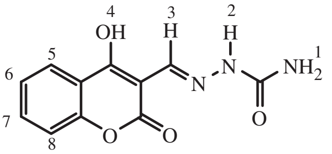

4-hydroxycoumarin-3-semicarbazone
HL^1

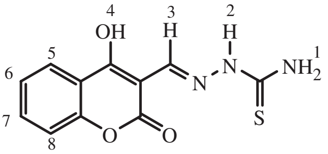

4-hydroxycoumarin-3-thiosemicarbazone
HL^2

Chemical shift, δ_{TMS} (ppm)/Assignment

HL^1	HL^2
10.55 s (H) hydrazide 2	11.29 s (H) hydrazide 2
17.07 s (H) phenolic 4	17.07 s (H) phenolic 4
7.2–7.7 m (5H); 4 CH coumarin 5-8 + CH hydrazide 3	7.2–7.7 m (5H); 4 CH coumarin 5-8 + CH hydrazide 3
6.20 s, (2H) amine 1	9.53 s, (2H) amine 1

s = singlet, m = multiplet.

tridendate ligands with phenolic-oxygen, azomethine-nitrogen, and the thio-keto or carbonyl-oxygen groups as ONO(S) ligands. The thiocarbazone exists as the thio-keto form since it has a –NH–C=S thio amide group, although in many instances thiol form or equilibrium mixture of both forms has been observed in thiosemicarbazones.

The ^{1}H NMR data of the ligands are collected in table 2. A signal is observed in both spectra at $\delta = 17.07$ ppm assigned for the phenolic OH [31, 32]. While the hydrazide proton of the CH attached to the coumarin moiety has shifted downfield toward the coumarin CH protons, the CH hydrazide proton, neighboring to the keto and the thio-keto groups, is observed at $\delta = 10.55$ and 11.29 ppm, respectively. The signals observed at $\delta = 6.20$ and 9.53 ppm are assigned for the NH_2 in the spectra of semi- and thiosemicarbazones, respectively [31, 32]. The protons of the coumarin are in the range $\delta = 7.2$–7.7 ppm [31, 32]. Addition of D_2O results in diminishing the signals due to the phenolic OH group. The signal due to S–H (thiol) is not observed in the expected range 2–3 ppm [31, 32], indicating that the ligand is in the thione form.

The UV-vis spectra recorded for ethanolic solutions of the ligands showed absorption bands in the range 260–300 nm assigned for π–π^* transitions within the coumarin and hydrazide, H–C=C–. Generally, the absorption is intensive and several bands of different complexity were seen up to about $\lambda \approx 400$ nm. The absorption bands observed in the range 320–350 nm could be attributed to the n–π^* transitions of the C=N (azomethine), C=O (coumarin), and the ketonic C=O or thio-keto C=S group. The complex absorption at $\lambda > 395$ nm is assigned for CT transitions encroaching on the visible region and giving the ligands their colors [31, 32].

The mass spectra of the ligands showed molecular ion peaks at $m/e = 247$ (20%) and 263 amu (15%) which coincide with formula weights for the HL^1 and HL^2, respectively. The base peak observed in both spectra at $m/e = 171$ amu corresponded to the ion $[C_{10}H_5NO_2]^+$. The spectra showed that the ligands underwent similar fragmentation behavior [31, 32].

3.2. *Metal complexes*

All the complexes have good solubility in DMF and DMSO but were insoluble in ether, water, acetone, and benzene. All the complexes are amorphous powders, stable at room temperature without decomposition on standing for several months. The molar conductance values of the complexes in DMF are presented in table 1. The values are too low to account for any dissociation and the complexes are considered to be nonelectrolytes [33].

3.3. *Infrared spectra*

The elemental analysis data of the metal complexes obtained (table 1) are in agreement with the formula given. The binding mode of the ligands to metal ions was further elucidated by analysis of the IR spectra (table 3) of ligands and their metal complexes. Comparison of infrared spectra of free ligands and their metal complexes (table 3) imply that these Schiff bases are monobasic tridentate ligands with the metal ion coordinated through the deprotonated oxygen atom of the phenolic, the nitrogen atom of the azomethine and the oxygen atom of the ketonic group in HL^1 or the sulfur atom of thio-keto group in HL^2.

The IR spectra of the metal complexes revealed absorption bands associated with the $\nu(O-H)$ of the phenolic groups (observed at $3340\,cm^{-1}$ in the free ligands) disappeared, indicating loss of phenolic proton on complexation and formation of metal-oxygen bonds. The $\delta(COH)$ mode [34–36] which appeared at $1355\,cm^{-1}$ in the spectrum of the ligand was not observed in the spectra of the complexes and supports the suggestion that the ligands coordinate through their deprotonated form. The presence of coordinated water was suggested by the very broad absorption centered around $3450\,cm^{-1}$ in the infrared spectra. Bands at 930 and $770\,cm^{-1}$ may be attributed to rocking and wagging modes of coordinated water [37–39].

Furthermore, the bands observed at 3270 and $1740\,cm^{-1}$ in the free ligand have been assigned to $\nu(NH)$ and $\nu(C{=}O)_{coumarin}$ vibrations, respectively. Practically no effect on these frequencies after complexation indicates noninvolvement of these groups in coordination. The most notable change in the ligands spectral features when coordinated to metal ion is the C=N red shift. The $\nu(C{=}N)$ band [36–39] at $1570\,cm^{-1}$ in the ligands exhibited a red shift of $\sim$40–$50\,cm^{-1}$ in the spectra of the complexes, evidence for participation of the C=N group in coordination to the metal ions.

A medium band at $1120\,cm^{-1}$ which is assigned to $\nu(N–N)$ in spectra of the ligands is shifted to the higher frequency in the spectra of all complexes. This shift on hydrazinic nitrogen indicates the presence of electron-withdrawing substituents [36–40]. However, in metal complexes the band shifts to higher wave number and splits, the result of increase in the multiplicity of the C–N bond. The strong bands at 1680 and $876\,cm^{-1}$ in spectra of HL^1 and HL^2, mainly due to stretching vibrations of (C=O) and (C=S), respectively, are shifted to lower frequency, 1630–1590 and 850–$820\,cm^{-1}$, respectively, in the corresponding spectra of the metal complexes indicating the coordination of ketonic-oxygen and the thio-keto sulfur to metal atom [39–41].

The possibility of thione-thiol tautomerism (H–N–C=S), ($C{=}N\cdot SH$) in the HL^2 ligand has been ruled out with no bands around 2700–$2500\,cm^{-1}$, characteristic of thiol

Table 3. Characteristic IR bands (cm^{-1}) of **HL^1** and **HL^2** and the corresponding metal complexes.

Compound	ν(C=N)	ν(N–H)	ν(N–N)	ν(C=O) Ketonic	ν(C=O) Coumarin	ν(OH), phenolic	ν(M–O)	ν(M–N)	ν(M–S)	Other bands
HL^1	1570 s	3270 m	1120 s	1680	1740	3340	–	–	–	δ$(COH)_{ip}$, 1355
(**1**) $[Co(L^1)(H_2O)_2(Cl)]$	1510 s	3265 m	1136 s	1640	1735	–	560 m	420 w	395 m	ν (3450); δ (930, 770) (coordinated H_2O)
(**2**) $[Co(L^1)(H_2O)_2(Br)]$	1525 m	3268 m	1137 w	1595	1740	–	540 m	425 w	375 m	ν (3450); δ (935, 770) (coordinated H_2O)
(**3**) $[Co(L^1)(H_2O)_2(NO_3)]$	1535 m	3270 s	1140 w	1595	1739	–	545 m	430 w	390 m	ν (3455); δ (930, 775) (coordinated H_2O)
(**4**) $[Ni(L^1)(H_2O)_2(Cl)]$	1510 m	3269 s	1125 w	1630	1738	–	555 m	410 w	385 m	ν (3436); δ (930, 775) (coordinated H_2O)
(**5**) $[Ni(L^1)(H_2O)_2(Br)]$	1515 m	3268 s	1136 s	1635	1740	–	560 w	445 w	395 m	ν (3438); δ (938, 770) (coordinated H_2O)
(**6**) $[Ni(L^1)(H_2O)_2(NO_3)]$	1520 m	3270 s	1140 w	1630	1735	–	555 w	445 w	375 m	ν (3430); δ (930, 770) (coordinated H_2O)
Compound	ν(C=N)	ν(N–H)	ν(N–N)	ν(C=S)	ν(C=O) Coumarin	ν(OH), phenolic	ν(M–O)	ν(M–N)	ν(M–S)	Other bands
HL^2	1570 s	3270 m	1120 s	876	1740	3332	–	–	–	δ$(COH)_{ip}$, 1355
(**7**) $[Co(L^2)(H_2O)_2(Cl)]$	1515 s	3265 m	1136 s	829	1735	–	560 m	430 w	385 m	ν (3450); δ (930, 770) (coordinated H_2O)
(**8**) $[Co(L^2)(H_2O)_2(Br)]$	1525 m	3268 M	1137 w	820	1740	–	550 m	420 w	375 m	ν (3450); δ (935, 770) (coordinated H_2O)
(**9**) $[Co(L^2)(H_2O)_2(NO_3)]$	1535 m	3270 s	1140 w	829	1739	–	545 m	435 w	390 m	ν (3455); δ (930, 775) (coordinated H_2O)
(**10**) $[Ni(L^2)(H_2O)_2(Cl)]$	1510 m	3269 s	1125 w	839	1740	–	555 m	410 w	395 m	ν (3436); δ (930, 775) (coordinated H_2O)
(**11**) $[Ni(L^2)(H_2O)_2(Br)]$	1515 m	3268 s	1136 s	850	1740	–	550 w	440 w	395 m	ν (3438); δ (938, 770) (coordinated H_2O)
(**12**) $[Ni(L^2)(H_2O)_2(NO_3)]$	1530 m	3270 s	1140 w	820	1735	–	550 w	445 w	365 m	ν (3430); δ (930, 770) (coordinated H_2O)

infrared absorption [38–41]. New bands at 560–375 cm^{-1} are tentatively assigned to ν(M–O), ν(M–N) and ν(M–S) (metal–ligand) stretching bands [41].

In the nitrate complexes, the absence of the ν_3 band of ionic nitrate (D_{3h}) around 1360 cm^{-1} and the occurrence of two strong bands at 1510 and 1300 cm^{-1} due to the split ν_3 mode indicate a coordinated nitrato group [42–47]. The number and relative energies [44] of nitrate combination frequencies ν_1 and ν_4 may be used to distinguish the various coordination modes of the nitrate group. If the $\nu_4 - \nu_1$ difference is taken as an approximate measure of the covalency of nitrate [44–46], a value of ~200 cm^{-1} suggests bidentate nitrate [44–47]. Investigation of the spectra of a number of compounds of known crystal structure shows the difference between ν_4 and ν_1 in the range ~206–216 cm^{-1}, indicating bidentate or bidentate chelating nitrate. Devi *et al.* [46] showed this to be true with separation of monodentate nitrate groups of 5–26 cm^{-1} and bidentate groups of 25–66 cm^{-1}. By applying this method, a separation of 15–20 cm^{-1} in the combination bands ν_1 and ν_4 indicate the monodentate nitrate coordination.

In conclusion, the infrared spectral studies suggest monobasic tridentate ligands with ONO(S) coordination sites from phenolic OH, azomethine and ketonic-oxygen or thio-keto groups.

3.4. *Mass spectrum of [Ni(ligand)(OH$_2$)$_2$Cl]*

The mass spectrum of the Ni(II) complex of HL^1, $[Ni(C_{11}H_8N_3O_4)(H_2O)_2Cl]$, showed the molecular ion at $m/e = 376$ amu. The fragments observed at $m/e = 340$ (20%) and 303 (35%) amu corresponded to $[Ni(C_{11}H_8N_3O_4)Cl]^+$ and $[Ni(C_{11}H_7N_3O_4)]^+$, respectively, in accordance with the results obtained from the thermal analyses (see thermal studies). The base peak fragment observed at $m/e = 229$ amu corresponded to $[Ni(C_{10}H_5NO_2)]^+$.

3.5. *Magnetic susceptibility*

The observed magnetic moments of cobalt(II) complexes of HL^1 and HL^2 are given in table 1. The theory of magnetic susceptibility of cobalt(II) ion was given originally by Schlapp and Penney [47] and the best summary of the magnetic behavior of cobalt compounds is that of Figgis and Nyholm [48]. The observed values of magnetic moment for cobalt(II) complexes are generally diagnostic of the coordination geometry about the metal ion. Low-spin square-planar cobalt(II) complexes are 2.9 B.M. arising from one unpaired electron plus an apparently large orbital contribution [48]. Both tetrahedral and high-spin octahedral cobalt(II) complexes possess three unpaired electrons but may be distinguished by the magnitude of the deviation of μ_{eff} from the spin-only value. The magnetic moment of tetrahedral cobalt(II) complexes with an orbitally nondegenerate ground term is increased above the spin-only value via contribution from higher orbitally degenerate terms and occurs in the range 4.2–4.7 B.M. [49]. Octahedral cobalt(II) complexes, however, maintain a large contribution due to ^4T_g ground term and exhibit μ_{eff} in the range 4.8–5.6 B.M. [49, 50]. The magnetic measurements on the complexes reported herein, 4.8–5.3 B.M., show that all are paramagnetic with three unpaired electrons in a high-spin octahedral configuration.

Magnetic behavior of octahedral nickel(II) complexes is relatively simple. Nickel(II) should exhibit a magnetic moment higher than expected for two unpaired electrons in octahedral, 2.8–3.2 B.M., and tetrahedral, 3.4–4.2 B.M., complexes, whereas its

Table 4. Electronic spectral data (cm^{-1}) and ligand field parameters of Co(II) complexes.

Complex	ν_1	ν_2 $^4T_{1g}(F) \rightarrow {}^4A_{2g}$	ν_3 $^4T_{1g}(F) \rightarrow {}^4T_{1g}(P)$	B (cm^{-1})	β	$10D_q$ (cm^{-1})	ν_2-ν_1 (cm^{-1})	ν_2/ν_1 (cm^{-1})
(**1**) $[Co(L^1)(H_2O)_2(Cl)]$	7385	15833	18770	829.87	0.740	8448	8448	2.14
(**2**) $[Co(L^1)(H_2O)_2(Br)]$	7397	15854	18785	829.87	0.740	8457	8457	2.14
(**3**) $[Co(L^1)(H_2O)_2(NO_3)]$	7390	15874	18790	832.93	0.740	8484	8484	2.15
(**4**) $[Co(L^2)(H_2O)_2(Cl)]$	7385	15833	18770	829.87	0.740	8448	8448	2.14
(**5**) $[Co(L^2)(H_2O)_2(Br)]$	7397	15854	18785	829.87	0.740	8457	8457	2.14
(**6**) $[Co(L^2)(H_2O)_2(NO_3)]$	7390	15874	18790	832.93	0.740	8484	8484	2.15

square-planar complexes would be diamagnetic. This increase in magnetic moment value from that of the spin-only value has been discussed by Nyholm [48] who considered it to be due to some "mixing in" of upper states via spin-orbit coupling. The paramagnetism observed for the present complexes ranges from 2.6–3.2 B.M. (table 1) consistent with octahedral stereochemistry.

3.6. *Electronic spectra*

3.6.1. Cobalt(II) complexes. The electronic spectra of the cobalt(II) complexes are very similar to each other and consist of two bands at 15,880 cm^{-1} ($^4T_{1g}(F) \rightarrow {}^4A_{2g}(F)$) ($\nu_2$) and 18,780 cm^{-1} ($^4T_{1g}(F) \rightarrow {}^4T_{1g}$ (P)) (ν_3), which clearly indicate the octahedral stereochemistry of the complexes. In table 4, the band maxima and their assignments and the calculated ligand field parameters are listed. The ligand field parameters $10D_q$ and B are calculated using first order perturbation theory [51, 52] and the transition energies are given by the following equations [51].

$$10D_q = \nu_2 - \nu_1$$

$$B = \frac{(\nu_2 + \nu_3 - 3\nu_1)}{15}$$

The methods of calculation of ligand field parameters from the ligand field spectra of octahedral Co(II) complexes have been discussed by Reedijk [52]. The energy of ν_1 corresponds to $10D_q$ for weak field complexes. With these assignments, B and D_q have been calculated (table 4).

3.6.2. Nickel(II) complexes. The electronic spectra of the complexes are very similar to each other with three bands at ~9090 cm^{-1} due to $^3A_{2g} \rightarrow {}^3T_{2g}(\nu_1)$, ~14,800 cm^{-1} due to $^3A_{2g} \rightarrow {}^3T_{2g}(\nu_2)$, and ~25,000 cm^{-1} for $^3A_{2g} \rightarrow {}^3T_{2g}(\nu_3)$ [48–51], which clearly indicate the octahedral stereochemistry. The relative strength of the ligand and geometry of the complexes can be illustrated by calculating the ligand field splitting parameters, $10D_q$ and B. In table 5, the band maxima and their assignments and the calculated ligand field parameters are listed [53, 54]. The method below was followed to determine $10D_q$ and B in the nickel(II) complexes.

$$10D_q = \nu_1$$

$$B = \frac{(\nu_2 + \nu_3 - 3\nu_1)}{15}$$

Table 5. Electronic spectral data (cm^{-1}) and ligand field parameters of Ni(II) complexes.

Complex	$\nu_1(10D_q)$ $^2A_{2g} \rightarrow {}^3T_{2g}(F)$	ν_2 $^3A_{2g} \rightarrow {}^3T_{2g}(F)$	ν_2 $^2A_{2g} \rightarrow {}^3T_{2g}(F)$	B (cm^{-1})	β	$10D_q$ (cm^{-1})	$\nu_2 - \nu_1$ (cm^{-1})	ν_2/ν_1 (cm^{-1})
(**7**) $[Ni(L^1)(H_2O)_2(Cl)]$	9090	14945	25000	845.00	0.79	9090	5855	1.64
(**8**) $[Ni(L^1)(H_2O)_2(Br)]$	9090	14945	25500	878.33	0.79	9090	5855	1.64
(**9**) $[Ni(L^1)(H_2O)_2(NO_3)]$	9100	14805	25500	867.00	0.79	9100	5705	1.63
(**10**) $[Ni(L^2)(H_2O)_2(Cl)]$	9090	14945	25000	845.10	0.79	9090	5855	1.64
(**11**) $[Ni(L^2)(H_2O)_2(Br)]$	9095	14945	25500	877.33	0.79	9095	5850	1.643
(**12**) $[Ni(L^2)(H_2O)_2(NO_3)]$	9100	14805	25500	867.00	0.79	9100	5705	1.63

3.7. *Thermal analyses*

Thermal decomposition data of two representative complexes, **4** and **10**, are presented in table 6. The thermogravimetric curves suggest that both complexes contain two molecules of coordinated water, which is evident by loss in weight at ~175°C. Complexes **4** and **10** showed second decomposition steps in the range ~250–450°C in which the complexes lose HCl, NH_2CO (or NH_2CS), N_2 and CO moieties. There is no change up to ~450°C; after that the rest of the organic ligand began to decompose at ~550°C. Finally, at ~670°C, metal oxide formed [39–41]. Based on the above results, the structures in figure 2 are suggested for the metal complexes.

3.8. *Antimicrobial activities*

A number of authors [19–23] have investigated the biological and medicinal properties of transition metal complexes of thiosemicarbazones. Thomas and Parmeswaran [20] studied the antitumor activities of Mn(II), Co(II), Ni(II), and Cu(II) chelates of anthracene-9-carboxaldehyde thiosemicarbazone. Murthy and Dharmaraja [21] reported the cytotoxic activity of phenylglyoxal bis(thiosemicarbazone) against *Ehrlich ascites* carcinoma cells. These compounds were also screened for antimicrobial activity on *B. subtilis* and *E. coli*, inhibiting bacterial growth considerably.

The Schiff bases, HL^1 and HL^2, and their metal complexes reported were evaluated for antimicrobial activity against one strain Gram +ve bacteria (*Staphylococcus aureus*) (**a**), Gram -ve bacteria (*Escherichia coli*) (**b**), fungus (*Candida albicans*) (**c**) and fungus *Fusarium solani* (**d**). The obtained results are presented in table 7. The Schiff base HL^1 was found to be biologically active; HL^2 showed remarkable antimicrobial activity which is expected as it contains sulfur. The table also shows that all metal complexes exhibit antimicrobial activity against one or more strains and enhanced compared with the parent Schiff bases. Remarkable enhancement was found for the complexes of HL^2.

Chelation tends to make the ligand a more potent bactericidal agent. A possible explanation for this increased activity upon chelation is that in chelated complex, the positive charge of the metal is partially shared with the donor atoms on the ligands and there is electron delocalization over the whole chelate ring. This, in turn, increases the lipophilic character of the metal chelate, favoring its permeation through the lipoid layers of the bacterial membranes. Generally, chelated complexes deactivate various cellular enzymes, which play a vital role in metabolic pathways of these micro-organisms. Other factors such as solubility, conductivity and dipole moment, which are

Table 6. Thermal decomposition data for $[Ni(L^1)(H_2O)_2(Cl)]$ and $[Ni(L^2)(H_2O)_2(Cl)]$.

Compound	Decomp. stage	Temp. range (°C)	% loss weight Found/(calcd)	DSC peak (°C)		ΔH (J/g)	Decomposition reaction
				Endo	Exo		
(**4**) $[Ni(L^1)(H_2O)_2(Cl)]$ $C_{11}H_{12}N_3O_6ClNi$ (376.2)	I	50–250	9.66 (9.57)	–	175	−120.83	$[Ni(L^1)(H_2O)_2(Cl)] \rightarrow [Ni(L^1)(Cl)] + 2H_2O$
	II	250–290	9.83 (9.70)	286	–	15.66	$[(Ni(L^1)(Cl)] \rightarrow [Ni(L^1 - H)] + HCl$
	III	290–370	16.31 (15.95)	–	369	−11.78	$[(Ni(L^1 - H))] \rightarrow [C_{10}H_3NO_3Ni)] + NH_2CONH_2$
	IV	370–450	23.34 (22.86)	375	–	14.84	$[C_{10}H_3NO_3Ni] \rightarrow [C_7H_2ONi] + HCN + 2CO$
	VI	450–550	The complex underwent decomposition processes until the formation of the metal oxide (NiO) at 678°C				
(**10**) $[Ni(L^2)(H_2O)_2(Cl)]$ $C_{11}H_{12}N_3O_5SClNi$ (392.2)	I	50–250	9.35 (9.16)	184	–	57.33	$[Ni(L^2)(H_2O)_2(Cl)] \rightarrow [Ni(L^2)(Cl)] + 2H_2O$
	II	250–290	9.17 (9.28)	–	265	−123.31	$[Ni(L^2)(Cl)] \rightarrow [Ni(L^2 - H)] + HCl$
	III	290–370	17.51 (17.14)	351	–	5.87	$[Ni(L^2-H)] \rightarrow [C_{10}H_3NO_3Ni] + NH_2CSNH_2$
	IV	370–450	21.45 (21.11)	377	–	14.84	$[C_{10}H_3NO_3Ni] \rightarrow [C_7H_2ONi] + HCN + 2CO$
	VI	450–550	The complex underwent decomposition processes until the formation of the metal oxide (NiO) at 670°C				

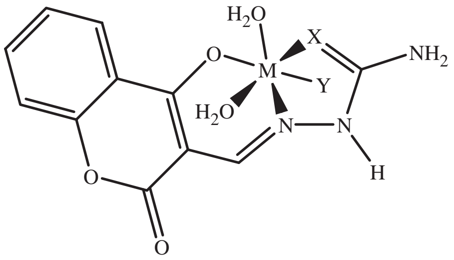

Octahedral schiff base HL^1 and HL^2 complexes
X = S or O; M = Co(II) or Ni(II) and Y = Cl$^-$, Br$^-$ or NO$_3$$^-$

Figure 2. Suggested structures of the metal complexes.

Table 7. Antimicrobial activity of the Schiff bases **HL^1** and **HL^2** and their metal complexes.

	Microbial species			
Compound	(**a**)	(**b**)	(**c**)	(**d**)
HL^1	+++	++	+++	+++
(**1**) [Co(L^1)(H$_2$O)$_2$(Cl)]	+++	+++	++	+++
(**2**) [Co(L^1)(H$_2$O)$_2$(Br)]	+++	+++	++	++
(**3**) [Co(L^1)(H$_2$O)$_2$(NO$_3$)]	+++	++	++	+++
(**4**) [Ni(L^1)(H$_2$O)$_2$(Cl)]	+++	+++	+++	+++
(**5**) [Ni(L^1)(H$_2$O)$_2$(Br)]	++	+++	+++	+++
(**6**) [Ni(L^1)(H$_2$O)$_2$(NO$_3$)]	+++	+++	++	++
HL^2	++++	+++	+++	++++
(**7**) [Co(L^2)(H$_2$O)$_2$(Cl)]	+++	+++	+++	+++
(**8**) [Co(L^2)(H$_2$O)$_2$(Br)]	++++	+++	++	++
(**9**) [Co(L^2)(H$_2$O)$_2$(NO$_3$)]	++++	+++	+++	+++
(**10**) [Ni(L^2)(H$_2$O)$_1$(Cl)]	++++	++++	+++	+++
(**11**) [Ni(L^2)(H$_2$O)$_2$(Br)]	++++	++++	++++	++++
(**12**) [Ni(L^2)(H$_2$O)$_2$(NO$_3$)]	+++	++++	+++	+++
Cephalosporin[a]	++++	+++	+++	++++
Streptomycin[b]	++++	+++	+++	++

(**a**) *S. aureus*, (**b**) *E. coli*, (**c**) *Candida albicans*, (**d**) *Fusarium solani*. Inhibition zone diameter in nm (% inhabitation): +, 8-10 (36–45%); ++, 10–16 (45–73%); +++, 16–19 (73–86); ++++, 19–22 (86–100%). Percent inhabitation values are relative to inhabitation zone (22 mm) with 100% inhabitation.
[a]Standard antifungal and [b]Antibacterial agents.

affected by the presence of metal ions, may also be reasons for increasing biological activity of the metal complexes compared to the ligand from which they are derived.

4. Conclusion

In the present studies, the Schiff bases, HL^1 and HL^2, coordinate to Co(II) and Ni(II) as monobasic tridentate ligands. The magnetic and electronic spectral studies suggest octahedral geometry of all complexes and the metal complexes enhanced antimicrobial activity in comparison to the free ligands.

References

[1] L. Driss, F. Ouidad. *J. Nat. Prod.*, **54**(2), 576 (1991).

[2] M.E. Marshall, J.L. Mohler, K. Edmonds. *J. Cancer Res. Clin. Oncol.*, **120**, S39 (1994).

[3] E. Moran, E. Prosser, R. O'Kennedy, R.D. Thornes. *J. Ir. Coll. Physicians Surg.*, **22**, 41 (1993).

[4] C.P. Siegers, H.C. Bostelmann. *J. Ir. Coll. Physicians Surg.*, **22**, 47 (1993).

[5] R.B. Myers, M. Parker, W.E. Grizzle. *J. Cancer Res. Clin. Oncol.*, **120**, S11 (1994).

[6] G. Feuer, J.A. Kellen, K. Kovac. *J. Cancer Res. Clin. Oncol.*, **33**(1), 35 (1976).

[7] D. Thornes, L. Daly, G. Lynch. *Eur. J. Surg. Oncol.*, **15**(5), 431 (1989).

[8] B. Omarbasha, W.R. Fair, W.D. Heston. *Cancer Res.*, **49**(11), 3045 (1989).

[9] L.D. Raev, E. Voinova, I.C. Ivanov. *Die Pharmazie*, **45**(9), 696 (1990).

[10] S. Sukdolaka, N. Vukovic, S. Solujic, M.Milosev, N. Manojlovic, L.J. Krstic. *J. Serb. Chem. Soc.*, **71**(6), 581 (2006).

[11] R.D. Thornes, L. Daly, G. Lynch. *J. Cancer Res. Clin. Oncol.*, **120**, S32 (1994).

[12] M.E. Marshall, K. Butler. *Mol. Biother.*, **3**(3), 170 (1991).

[13] M.A. Al-Haiza, M.S. Mostafa, M.Y. El-Kady. *Molecules*, **8**, 275 (2003).

[14] H. Kolodziej, O. Kayser, H.J. Woerdenbag, W. van Uden. *Zeitschrift für Naturforschung C*, **53**(3–4), 240 (1997).

[15] D. Jiang, R. Deng, J. Wu. *Wuji Huaxue*, **5**, 21 (1989).

[16] R. Deng, J. Wu, L. Long. *Bulletin des Sociétés Chimiques Belges*, **101**, 439 (1992).

[17] S.B. Padhy, G.B. Kauffman. *Coordination Chemistry Reviews*, **63**, 127 (1985).

[18] D.X. West, S.B. Padhy, P.B. Sonawane, R.C. Chikte. *Structure & Bonding*, **76**, 1 (1991).

[19] D.X. West, S.B. Padhy, P.B. Sonawane, R.C. Chikate. *Asian Journal of Chemistry Reviews*, **4**(1), 125 (1990).

[20] A.K. Nandi, S. Chaudhri, S.K. Mazumdah, S. Ghosh. *J. Chem. Soc. Perkin Trans.*, **11**, 1729 (1984).

[21] M.A. Ali, D.A. Chowdhary, M. Naziruddin. *Polyhedron*, **3**(5), 595 (1984).

[22] J.P. Scovill, D.L. Klayman, C.F. Franchino. *J. Med. Chem.*, **26**(10), 1261 (1982).

[23] M.E. Hossain, M.N. Alam, J. Begum. *Inorg. Chim. Acta.*, **29**(2), 207 (1996).

[24] P. Bindu, M.R.P. Kurup, T.R. Satyakeerty. *Polyhedron*, **18**(3-4), 321 (1999).

[25] R.K. Agarwal, G. Singh, B. Bhushan. *Polish J. Chem.*, **68**, 871 (1994).

[26] R.K. Agarwal, S. Prasad, N. Gahlot. *Turk. J. Chem.*, **28**(6), 691 (2004).

[27] S.S. Salah. *Ind. Eng. Chem. Res.*, **40**(1), 37 (2001).

[28] A.I. Vogel. *Textbook of Quantitative Inorganic Analysis*, 4th Edn, p. 338, Longman, London (1978).

[29] M.B. Ferrari, S. Capacchi, G. Pelosi, P. Tarasconi, R. Alberitini, S. Pineli, P. Lunghi. *Inorg. Chim. Acta*, **286**, 134 (1999).

[30] C.H. Colins, P.M. Lyne. *Microhiul Melfwds*, p. 422, University Park Press, Baltimore (1970).

[31] D. Williams, D.H. Fleming. *Spectroscopic Methods in Organic Chemistry*, p. 94, McGraw-Hill, New York (1966).

[32] R.M. Silverstein, G.C. Bassler, T.C. Morrill. *Spectrometric Identification of Organic Compounds*, John Wiley & Sons, New York (1991).

[33] W.J. Geary. *Coord. Chem. Rev.*, **7**(1), 81 (1971).

[34] P.W. Sadler. *J. Chem. Soc.*, 957 (1961).

[35] P.S. Radhakrishnan, P. Indrasenan, C.G.R. Nair. *Polyhedron*, **3**(1), 67 (1984).

[36] A. Yamguchi, R.B. Penland, S. Mizushima, T.J. Lane, C. Curran, J.V. Quagliano. *J. Am. Chem. Soc.*, **80**, 527 (1958).

[37] K. Swaminathan, H.M.N.H. Irving. *J. Inorg. Nucl. Chem.*, **26**(7), 1291 (1964).

[38] R.K. Agarwal, N. Goel, A.K. Sharma. *J. Indian Chem. Soc.*, **78**, 39 (2001).

[39] V.B. Rana, P.C. Jain, M.P. Swami, A.K. Srivastava. *J. Inorg. Nucl. Chem.*, **37**, 1826 (1975).

[40] J.E. Stewart. *J. Chem. Phys.*, **26**, 248 (1957).

[41] K. Nakamoto. *Infrared Spectra of Inorganic and Coordination Compounds*, John Wiley & Sons, New York (1970).

[42] N.M. Karayannis, C.M. Mikulski, L.L. Pytlewski, M.M. Labes. *Inorg. Chem.*, **13**, 1146 (1974).

[43] C.C. Addison, N. Logan, S.C. Wallwork, C.D. Garner. *Reviews of the Chemical Society*, **25**(2), 289 (1971).

[44] R.E. Heter, W.E.L. Grossman. *Inorg. Chem.*, **5**, 1308 (1966).

[45] J.R. Ferraro. *J. Mol. Spectrosc.*, **4**, 99 (1960).

[46] G.S. Devi, P. Indrasenan. *Inorg. Chim. Acta*, **133**, 157 (1987).

[47] R.K. Agarwal, D. Sharma, L. Singh, H. Agarwal. *Bioinorg. Chem. Appl.*, **2006**, 1 (2006).

[48] B.N. Figgis, R.S. Nyholm. *J. Chem. Soc.*, 4190 (1958).

[49] B.N. Figgs, *Introduction to Ligand Field*, Wiley, New York (1966); A.B.P. Lever. *Inorganic Electronic Spectroscopy*, 2nd Edn, Elsevier, Amsterdam (1984).

[50] S. Yamada. *Chem. Rev.*, **1**(14), 415 (1966).
[51] A.B.P. Lever. *J. Chem. Educ.*, **45**, 711 (1981).
[52] J. Reedijk, W.L. Driessen, W.L. Groeneveld. *Recueil des Travaux Chimiques des Pays-Bas.*, **88**, 1095 (1969).
[53] Y. Tanabe, S. Sugano. *J. Phys. Soc. Jpn.*, **9**(5), 753 (1954).
[54] Y. Tanabe, S. Sugano. *J. Phys. Soc. Jpn.*, **9**(5), 766 (1954).